Accepted Manuscript

Design, synthesis and antitrypanosomal activity of some nitrofurazone 1,2,4-triazolic bioisosteric analogues

Fredson T. Silva, Caio H. Franco, Denize C. Favaro, Lucio H. Freitas-Junior, Carolina B. Moraes, Elizabeth I. Ferreira

PII: S0223-5234(16)30358-0

DOI: 10.1016/j.ejmech.2016.04.065

Reference: EJMECH 8580

To appear in: *European Journal of Medicinal Chemistry*

Received Date: 14 January 2016

Revised Date: 25 April 2016

Accepted Date: 26 April 2016

Please cite this article as: F.T. Silva, C.H. Franco, D.C. Favaro, L.H. Freitas-Junior, C.B. Moraes, E.I. Ferreira, Design, synthesis and antitrypanosomal activity of some nitrofurazone 1,2,4-triazolic bioisosteric analogues, *European Journal of Medicinal Chemistry* (2016), doi: 10.1016/j.ejmech.2016.04.065.

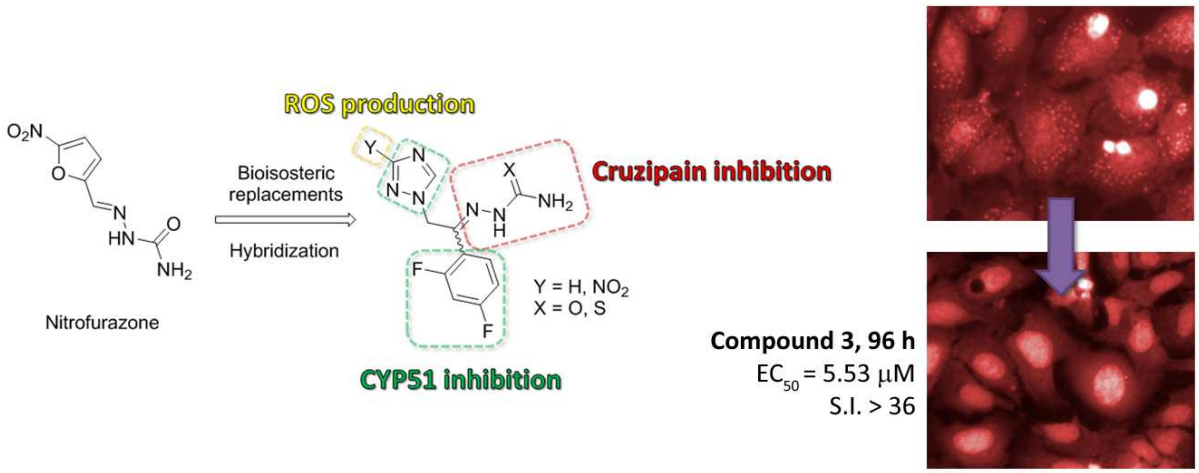

Design, synthesis and antitrypanosomal activity of some nitrofurazone 1,2,4-triazolic bioisosteric analogues

Fredson T. Silva[1], Caio H. Franco[2], Denize C. Favaro[3,4], Lucio H. Freitas-Junior[2], Carolina B. Moraes[2], Elizabeth I. Ferreira[1]*

1. School of Pharmaceutical Sciences, University of São Paulo, Avenida Prof. Lineu Prestes, 580, Bl. 13, São Paulo, São Paulo, Brazil

2. National Laboratory of Biosciences, National Center for Research on Energy and Materials, Rua Giuseppe Máximo Scolfaro, 10000, Campinas, São Paulo, Brazil

3. Institute of Chemistry, University of São Paulo, Avenida Prof. Lineu Prestes, 748, São Paulo, São Paulo, Brazil

4. Department of Chemistry, Institute of Exact Sciences, Federal University of Minas Gerais, Belo Horizonte, Brazil.

*Corresponding author: hajudan@usp.br

HIGHLIGHTS

- Four novel trypanomicidal non-toxic compounds are proposed.
- A novel compound showed promising EC_{50} value.
- The ratio of *Z* isomer of compounds increases with time due to mesomeric stabilization.

ABSTRACT

Chagas disease, caused by *Trypanosoma cruzi*, is a parasitosis that predominates in Latin America. It is estimated that 25 million people are under the risk of infection and, in 2008, more than 10 thousand deaths were registered. The only two drugs available in the therapeutics, nifurtimox and benznidazole, showed to be more effective in the acute phase of the disease. However, there is no standard treatment protocol effective for the chronic phase. Nitrofurazone (NF), an antimicrobial drug, has activity against *T. cruzi*, although being toxic. Considering the need for new antichagasic drugs, the existence of promising new therapeutic targets, as 14α-sterol demethylase and cruzain, and employing the bioisosterism and molecular hybridization approaches, four novel compounds were synthesized, characterized by melting point range, elemental analysis, IR and NMR spectroscopy. The compounds were tested against *T. cruzi* amastigotes in infected U2OS cells. All compounds showed selectivity towards *T. cruzi* and showed trypanomicidal activity in low micromolar range. The compound **3** showed potency similar to benznidazole, but lower efficacy. These results highlight the importance of the 1,2,4-triazole, thiosemicarbazonic and nitro group moieties for designing new efficient compounds, potentially for the chronic phase of Chagas disease.

KEYWORDS: Chagas disease; molecular hybridization; bioisosterism; nitroheterocyclic compounds.

INTRODUCTION

Chagas disease, also known as American trypanosomiasis, is an infectious disease caused by the protozoan *Trypanosoma cruzi*[1,2]. Predominantly present in Latin America, it is estimated to cause 7 thousand deaths yearly and approximately 7 million people are estimated of being infected worldwide. However, some studies have suggested that this number is underestimated due to failures on diagnosis and notification[3,4].

The acute stage of this illness is virtually asymptomatic and often difficult to detect, depending of the host's immune system[5]. The therapy mainly relies on nitroaromatic drugs, nifurtimox and benznidazole, which are responsible for 50 to 60% of parasitological cure of adults in the chronic stage and show considerable toxicity[6]. Therefore the search for new and more effective drugs is of utmost importance.

Finding an appropriate treatment for the chronic phase of Chagas disease has been a complex and difficult challenge. Despite many molecular targets have been explored, and high potency and low toxicity molecules are being found, the clinical trials did not succeed (Merck, ClinicalTrials.gov ID NCT01377480, *Hospital Universitari Vall d'Hebron Research Institute*, ClinicalTrials.gov ID NCT01162967). The differences among strains of the parasite and the complexity of the interactions between parasite and host can be responsible for those drawbacks[7].

It is worth mentioning nitrofurazone, a nitroheterocyclic topic antiseptic, which is known to have antitrypanosomal activity by generating oxygen reactive species, which interferes with trypanothione reductase[8,9], a specific parasite detoxifying enzyme, and also a inhibition of cruzipain, the main parasite protease[10]. The exploration of this dual mechanism is a strategy to

overcome the problems of low efficacy and parasite resistance during the chronic phase. Another approach includes the 1,2,4-triazole scaffold, that can interact with the parasitic CYP51 by coordinating the heterocyclic nitrogen to the iron atom of the CYP51 prosthetic heme group, thus inhibiting the synthesis of the parasitic cellular membranes[11,12,13].

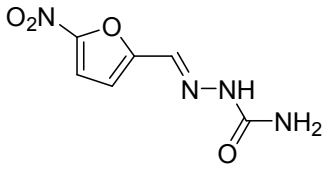

1

(caption removed)

Molecular modification is considered the most effective approach for developing new molecular entities[14]. Bioisosterism and molecular hybridization are among methods for achieving better pharmacokinetic and pharmacodynamic properties, and have been widely used on the search for novel bioactive compounds[15,16].

Considering the promising activity of triazolic CYP51 inhibitors as potential antichagasic agents, the use of nitroheterocyclic compounds on the Chagas disease treatment and the reported function of the thiosemicarbazone group as a potent cruzain inhibitor[17], we decided to use the mentioned moieties in a molecular hybridization approach, designing molecules similar to nitrofurazone for optimizing the biological profile.

In this work, we report the design, synthesis and the biological evaluation of four new compounds resulted from bioisosteric modifications of the furane ring and the hydrazone lateral chain of nitrofurazone. In addition, two intermediate synthesis have been submitted to the same biological evaluation.

RESULTS AND DISCUSSION

Synthesis

The designed molecules present a bioisosteric replacement of the furane ring to a 1,2-4-triazole system. The 1-*H*-1,2,4-triazole chemistry, especially the substitution on nitrogen 1, is well described in the literature due to its function in the pharmacophore group of azolic antifungals, such as fluconazole, itraconazole and voriconazole[18,19].

Synthesis of the aromatic hydrazones **4a, 4b**, **7a** and **7b** (Chart 1) required the preparation of the alkyl-1,2,4-triazoles **3** and **6**, respectively. The alkyl-1,2,4-triazoles were obtained by the nucleophile substitution of 2-Chloro-2',4'-difluoroacetophenone by the appropriate triazole in basic conditions and purified by chromatographic column. Ketones were mixed in reflux with the hydrazides in acidic conditions to afford the desired hydrazones. Nitrotriazole **2** was prepared by the oxidation of commercially available 3-amino-1,2,4-triazole, using the procedure described in literature[20].

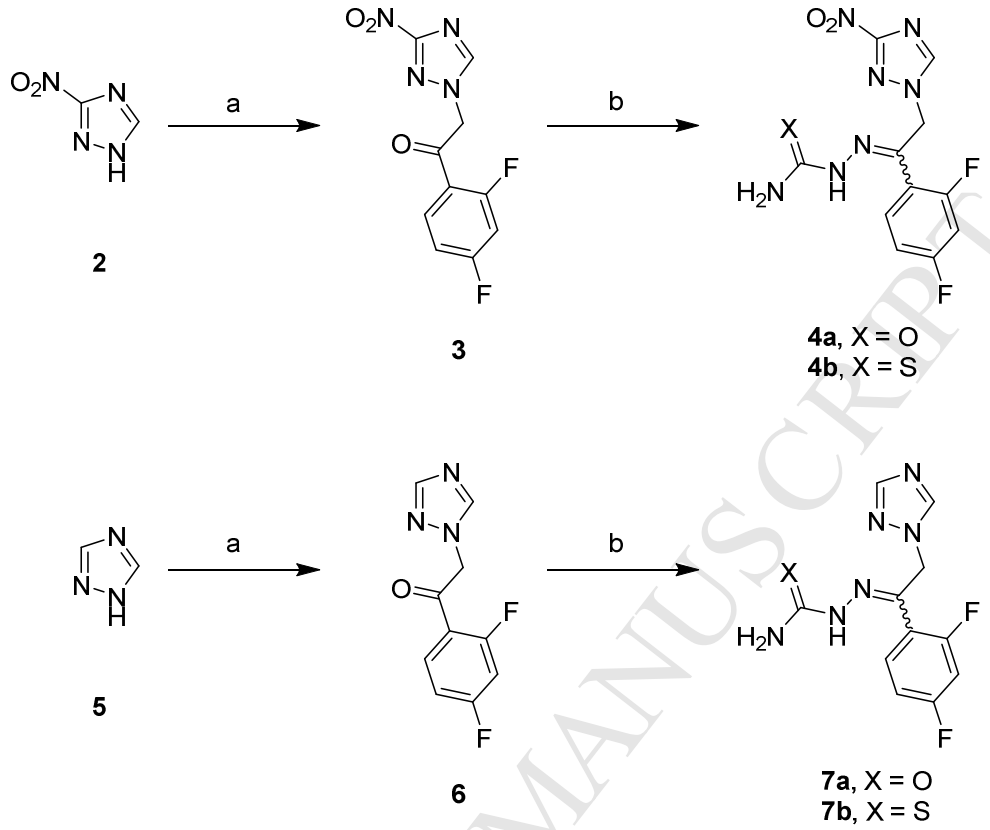

Chart 1. Synthetic route for obtaining nitrofurazone analogues. Reactions conditions: a) triazole sodium salt, acetonitrile, 2-Chloro-2′,4′-difluoroacetophenone, reflux; b) semicarbazide or thiosemicarbazide, ethanol, HCl, reflux.

All compounds were characterized by melting point, TLC, IR and NMR. The hydrazones were found to form a time dependent *E/Z*-equilibrium in solution and once formed could not be separated from the crude products by crystallization or column chromatography. Experimentally, it is unequivocal that the *E*-isomer is almost the only compound when the solution is fresh. In order to make the analysis of the diastereoisomeric population easier, the compound **4b** was used as reference (NMR experiments are presented in the Supporting Information).

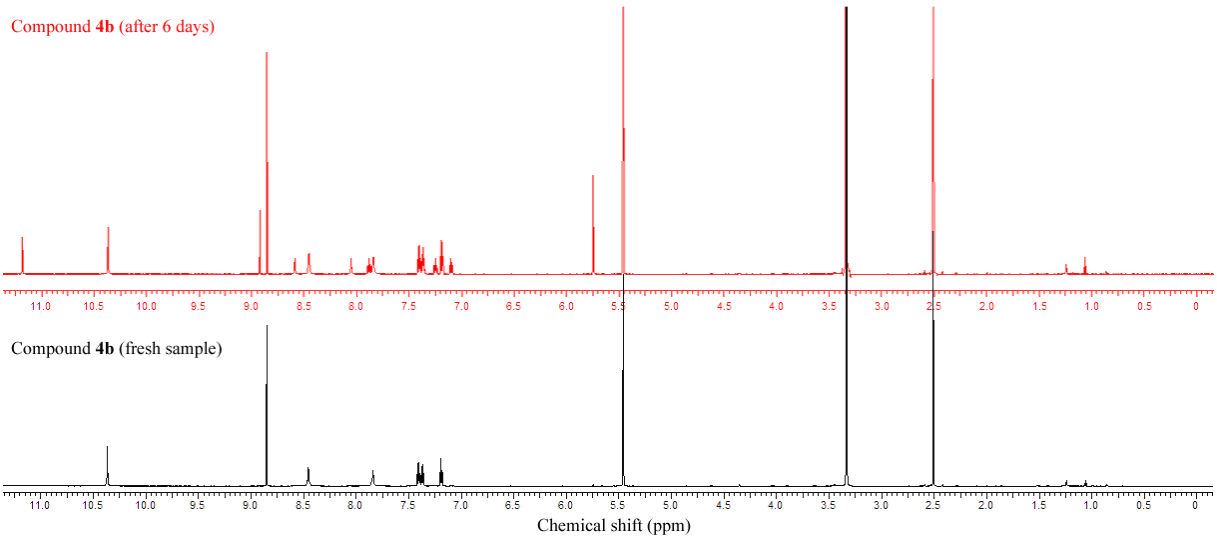

Figure 1. ^{1}H NMR spectra of compound **4b** using a fresh solution and 6 days later.

It was observed in the NOESY experiment that a distinct NOE interaction occurs between H-2 and H-3 for only one of the isomers, what is expected for the isomer that possesses shorter intramolecular distances (Table 1). For correct peak assignment and *E*/*Z* proportion calculation, the interatomic distance between H-2 and H-3 was calculated for both isomers of molecules **4a**, **4b**, **7a** and **7b** using the most stable conformers (see Computational analysis section).

Table 1. Interatomic distances between H-1 and H-3 on the studied hydrazones.

Compound	E (Å)	Z (Å)
4a	4.4	2.7
4b	4.5	2.3
7a	4.4	2.7
7b	4.4	2.7

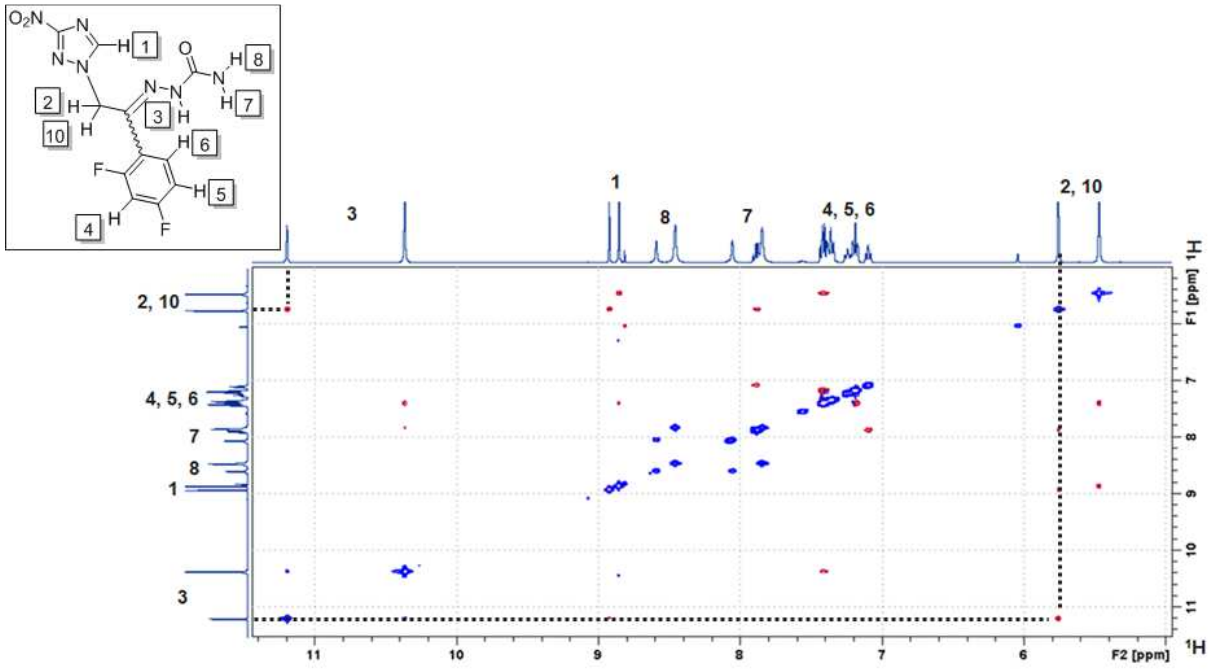

Figure 2. NOESY spectrum for compound **4b**. Distinctive correlations are depicted by dashed lines.

The formation of isomers during hydrazone synthesis is common and well described in the literature[21]. Separation of the isomers is often achieved using chromatography column, and structural characterization is performed separately when possible. However, some hydrazones present time-dependent interconversion when dissolved. Those compounds, even when isolated, may interconvert to the other configuration in biological fluids. This phenomenon is of particular interest of nanotechnology, using this conversion as molecular switches of molecular motors.[21] Conversely, regarding to small bioactive molecules, such behavior can difficult the determination of the favored bioactive configuration since the rate of isomerization may be dependent on biologic assay conditions.

Computational analysis

All energy minimizations calculations were performed using B3LYP/cc-pVTZ considering both an isolated molecule and taking into account the solvent effect. The most stable conformer of each isomer is shown in Table 2. Surprisingly, although *E* is the main reaction product, the calculations indicate that, thermodynamically, the *Z*-isomer is the most stable (Table 2). In this way, we left the fresh solution of **4b** in DMSO-d_6 for 6 days at room temperature, and after that we acquired the ^{1}H spectrum again. Unexpectedly, we observed that the population of the *E*-isomer has decreased while the population of the *Z*-isomer has increased along time (Figure 1). In the literature, we found that this fact is well documented for some semicarbazones; In 2013, Jakusová and collaborators[22] showed that, for isatin-3-(4-phenyl)semicarbazone and *N*-methylisatin-3-(4-phenyl)semicarbazone, the type and initial concentration of the reactants and the solvent of the reaction could affect the *E/Z* isomeric ratio. Besides, depending on the thermodynamic stability of the product a thermally or a photo chemically initiated isomerization can occur after its re-dissolution. In the occasion, the authors assumed, without a deep investigation, that the *Z*-isomer is more stable thermodynamically compared to *E* due to the existence of intramolecular hydrogen bonds.

Table 2. Free energy of the most stable conformers in DMSO for compound 4b, isomers *E and Z*, calculated at the B3LYP/cc-pVTZ theoretical level.

	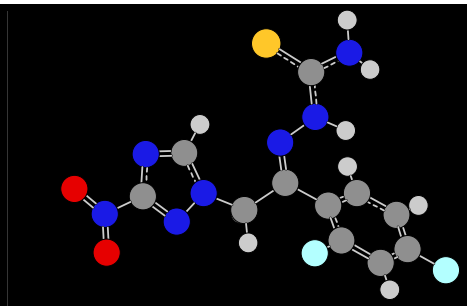 *E*-isomer	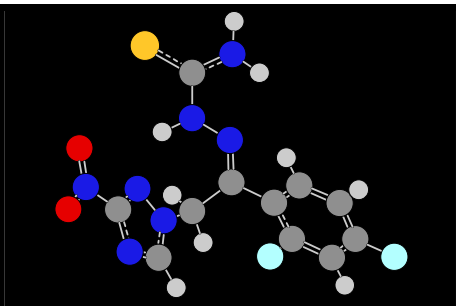 *Z*-isomer
ΔG (kcal/mol)	Isolated molecule	
	+7.7	0.00
	DMSO	
	+2.49	0.00

* According to results presented on Table S1 (Supporting Information), the *Z*-isomer is by far the most stable in the vacuum (ΔG > 5kcal/mol) and this difference decreases when the solvent effect is included.

Although this kind of isomerization has been reported previously, considering the practical application of our compounds, we decided to investigate the influence of stereoeletronic interactions [attractive (delocalization) or repulsive (steric interactions)] on this time dependent equilibrium and using the compound **4b** as reference, we performed Natural Bond Orbital (NBO)[23] analyses to explain the *Z*-isomer stability.

First, the NBO analysis of a full wave function was performed. The most important orbital interactions from the NBO analysis, responsible for the stabilization of the *Z*-isomer, are presented at Table 3. Surprisingly, the NBO analysis pointed out that only for the *Z*-isomer the mesomeric effect is effective. For the *E*-isomer the hyperconjugative interactions involving the nitrogen's lone pairs (LP) and the sigma antibonding orbital (σ^*_{CS}) constitute the most important interaction. So, in order to analyse the influence of the attractive and repulsive interactions on the

stability of the isomers, only the attractive delocalization interactions were deleted (NBOdel) and the energy of the isomers were recalculated. The energy change presented at Table 3 is the difference between the full molecular electronic energy and the molecular electronic energy calculated disregarding the attractive interactions. These values can be used to compute the amount of attractive or repulsive interactions in each isomer. The higher energy change for the *Z*-isomer demonstrates that for this isomer the repulsive interactions are bigger than in the *E*-isomer; meanwhile the attractive interaction, larger in the *Z*-isomer, overcomes the repulsive ones.

Table 3 displays the most important interactions from the NBO analysis involving the semicarbazone moiety of the two isomers. From this Table, the attractive interactions involving the semicarbazone moiety are larger for the *Z*-isomer. It is worth to mention that other interactions also contribute for the *Z*-isomer stabilization.

Table 3. Orbital interactions energies (kcal/mol) from NBO of a full wave function analysis and energies obtained from the NBO deletion calculation for *Z*- and *E*-isomer at the B3LYP/cc-pVTZ level.

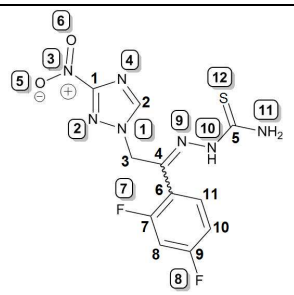

Orbital Interactions	*Z*	*E*
$LP(N_{11})\rightarrow\pi^*_{C5\text{-}S12}$	78.99	-
$LP(N_{10})\rightarrow\pi^*_{C5\text{-}S12}$	56.45	6.56
$LP(N_{10})\rightarrow\pi^*_{C4\text{-}N9}$	36.04	33.18
$LP(N_{10})\rightarrow\sigma^*_{C5\text{-}S12}$	-	32.59
$LP(N_{11})\rightarrow\sigma^*_{C5\text{-}S12}$	0.55	44.72
$LP(N_{2})\rightarrow\sigma^*_{N10\text{-}H3}$	2.79	-
$LP(N_{9})\rightarrow\sigma^*_{N11\text{-}H7}$	1.13	-
$LP(N_{9})\rightarrow\sigma^*_{N10\text{-}H3}$	8.28	9.28
Sum	184.23	126.33
Total SCF energy (a.u)	-1556.474193519	-1556.460129916
Deletion energy (a.u)	-1553.488265196	-1553.703426618
Energy change (a.u)*	2.985928	2.756703
ΔE (kcal/mol)**	143.8	0.0

* Energy change = Total SCF energy - Deletion energy (a.u). ** ΔE (kcal/mol) = [Energy change(*Z*) - Energy change(*E*)] x 627.5095.

Biological evaluation (In vitro* anti-*T. cruzi* evaluation*)

The antiparasitic activity of the synthetized nitrofurazone analogs was determined against intracellular amastigotes of the *Trypanosoma cruzi* Y strain in a High Content Screening (HCS) assay[7] in two sets of experiments. The results are shown in Table 4. The mean EC_{50} value of the reference compound benznidazole, in the low micromolar range (approximately 4 μM), and efficacy (maximum activity) of approximately 100%, are within the expected values, as previously reported, while the reference compound nifurtimox was slightly more potent, with a mean EC_{50} value of 0.39 μM[7,24,25]. Compounds **4b** and **7b** showed low potency against amastigotes, with EC_{50} values of approximately 22 and 15 μM, respectively, but were efficacious in reducing infection, with maximum activity values of 92 – 95%. Compound **3** was similar to benznidazole in potency, with an EC_{50} in the low micromolar range (5.53 μM), however it was not as efficacious, with a maximum activity of approximately 87%. Compound **4a** was far less potent than the others, with an EC_{50} value of approximately 100 μM, but efficacious nonetheless. Compounds **7a** was only moderately active, with a mean EC_{50} greater than 60 μM, but with levels of efficacy (max. active. of 96%) comparable to values observed for compounds 4a and 7b. Compound **6** was poorly active against *T. cruzi*, with an EC_{50} of 144 μM a maximum efficacy of approximately 68. None of the tested compounds displayed overt cytotoxicity on the host cells under the tested conditions, and all were selective towards *T. cruzi*, as suggested by the selectivity indexes obtained. The compounds were also assayed for cytotoxicity against non-infected U2OS, however no differences were observed in comparison with infected U2OS cells (data not shown).

It can be observed that the absence of the nitro group in compound **6** significantly impacted trypanocidal activity, as its nitro analogue **3** is 26-fold more potent. This indicates that the ROS

releasing mechanism predominates over the CYP51 inhibition in that kind of scaffold, independently on its resemblance to the antifungal azoles structure. Compound **3** can be considered a bioisoster of benznidazole, possibly acting via similar mechanisms. It has similar potency, but it is 3-fold less selective and its efficacy is 16% lower.

Otherwise, comparing the hydrazones **4** and **7**, it is observed that the removal of the nitro group resulted in a slightly enhanced activity. That difference may be related to the influence of hydrazone lateral chain on the nitro group oxidation potential. Thiosemicarbazone compounds **4b** and **7b** showed to be about 4-fold more potent than the semicarbazonic bioisosteres **4a** and **7a**.

Table 4. EC_{50}, CC_{50} and Selectivity Index (S.I.) values for nitrofurazone analogues and reference compounds against *T. cruzi* Y strain intracellular amastigotes

Compounds	**EC_{50} (μM)**	**CC_{50} (μM)**	**S.I.**	**Max. Actv. (%)**
Benznidazole	3.96	N.D.	> 101	103.5
Nifurtimox	0.34	26.8	78.9	101.5
3	5.53	N.D.	> 36	86.99
4a	101.30	N.D.	> 2	95.23
4b	21.57	N.D.	> 9.27	92.75
6	144	N.D.	> 1.4	68.7
7a	63.1	N.D.	> 3.1	96.6
7b	15.37	N.D.	> 13.01	95.22

Data obtained from three independent experiments. N.D. indicates that the mean value could not be calculated. S.I., selectivity index. Max. Actv., maximum normalized activity.

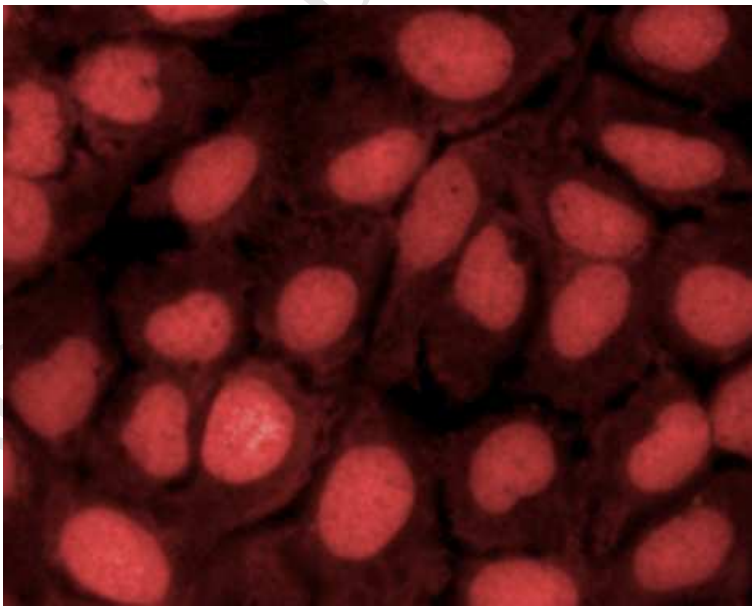

Figure 3. Positive control for activity.

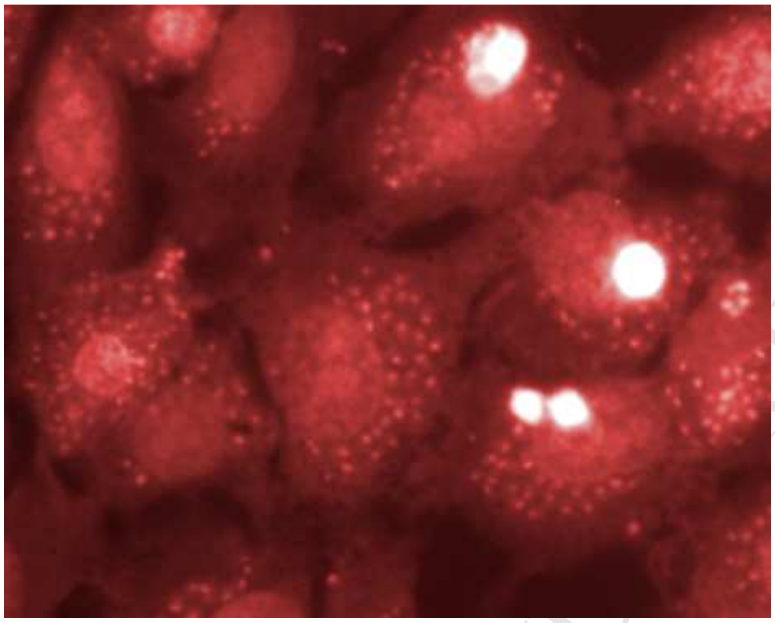

Figure 4. Negative control for activity (cells infected with *T. cruzi* amastigotes).

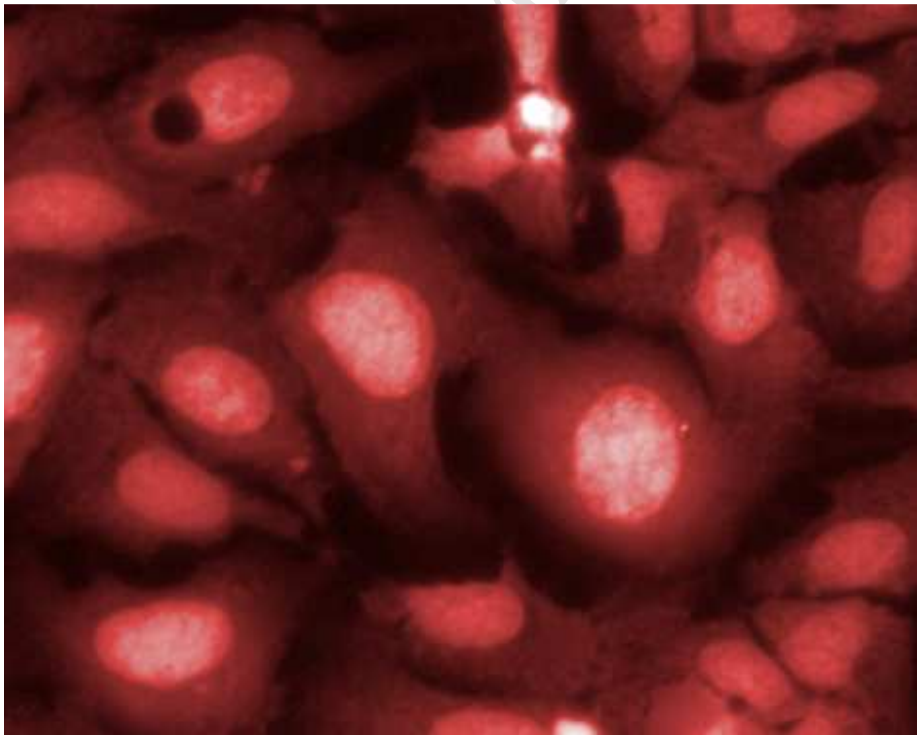

Figure 5. Non-infected U2OS cells after 96 h of exposure of compound **3.**

CONCLUSION

Four novel compounds were designed, synthesized and more two intermediates of synthesis had their antitrypanosomal activity evaluated in comparison with standard drugs benznidazole and nifurtimox. Due to the nature of the general scaffold, a triple mechanism of action: CYP51 inhibition, cruzain inhibition and ROS releasing, was expected.

The presence of thiosemicarbazonic group is considered important for the biological activity of the synthesized hydrazones, possibly by the inhibition of cruzain. The removal of nitro group did not cause total loss of activity, evidencing that this group of compounds acts by other mechanisms beyond the production of reactive oxygen species.

Compound **3** has potency similar to benznidazole, which has a very similar chemical structure, possibly acting by the same ROS releasing mechanism. This compound could be used as a scaffold for the design of new, more active and selective compounds. Enzymatic studies should be performed to elucidate the exact mechanism of action for better understanding the relationships between different targets and further structural optimizations.

EXPERIMENTAL SECTION

All starting materials were purchased from Sigma-Aldrich and were used without further purification. The progress of all reactions was monitored by Analytical thin-layer chromatography (TLC), which was performed on silica-gel 60 GF (5-40 μM thickness) plates. Visualization was accomplished with UV light. Melting points and decomposition temperatures were measured with an eletrothermal melting-point apparatus (Büchi, M-565 model) in open capillary tubes and are uncorrected. Automated flash column chromatography was carried out using a Biotage Isolera Prime (Biotage GB Limited, Hengoed, UK) with 25 g and 100 g SNAP

cartridges. Infrared experiments were performed on a Shimadzu FTIR spectrophotometer, using 5 mg samples for the preparation of KBr pellets. Wavelengths of maximum absorbance are quoted in wavenumbers (cm^{-1}). The ^{1}H, ^{13}C, HSQC, HMBC and NOESY experiments were performed on a Bruker Avance III NMR spectrometer in DMSO-*d6* at 300 MHz and 500 MHz. Chemical shifts (δ) are reported in ppm and are referenced to Me_4Si. Elemental analyses (C, H and N) were performed on a Perkin-Elmer model 2400 analyser, and the data were within 0.4% of the theoretical values.

General procedure for the synthesis of the alkyl-triazoles

The triazoles were converted to their sodium salts by treatment with an aqueous solution of sodium hydroxide followed by precipitation, according to the previous literature[26]. The reaction proceeded according to the procedure described by Papadopoulou et al.[27] After dried, the sodium salt of the respective triazole was solubilized in acetonitrile and added to an equimolar solution (0,5 M) of 2-Chloro-2',4'-difluoroacetophenone in acetonitrile for a nucleophilic substitution, which occurred under refluxing conditions (8 h). The resulting suspension was filtered, and the liquid phase was evaporated. The resulting solid was purified using automated flash column chromatography.

1-(2,4-difluorphenyl)-2-(3-nitro-1*H*-1,2,4-triazol-1-yl)ethane-1-one (**3**): Off-white powder, Yield, 46%. mp 113-114 ºC. IR (cm^{-1}): 1697 (C=O), 1609 (C=C), 1508 (Ar-NO_2). ^{1}H NMR (DMSO-d_6): 8.81 (s, 1H); 8.03-8.11 (m, 1H); 7.51-7.59 (m, 1H); 7.30-7.36 (m, 1H); 6.03 (s, 2H). ^{13}C NMR (DMSO-d_6): 187.96; 167.51; 164.37; 160.77; 148.31; 132.60; 119.23; 112.71; 105.40;

59.27. Anal. Calcd for $C_{10}H_6F_2N_4O_3$: C, 45.01; H, 2.30; N, 20.39. Found: C, 44.96; H, 2.32; N, 20.51.

General procedure for the synthesis of the hydrazones

The adequate ketone (10 mmol) and the respective hydrazide (10 mmol) were solubilized in anhydrous ethanol (10 mL) and mixed with 0,15 mL of hydrochloric acid. The mixture was stirred under reflux (12 h). The resulting solution was evaporated and the solid was purified using automated flash column chromatography.

2-(1-(2,4-difluorophenyl)-2-(3-nitro-1*H*-1,2,4-triazol-1-yl)ethylidene)hydrazine-1-carboxamide (**4a**): (E:Z proportion = 87:13) Off-white powder, Yield: 10%, temperature of decomposition: 140 ºC. IR (cm^{-1}): 1670 (C=O), 1617 (C=N), 1504 (C=C Ar). ^{1}H NMR (DMSO-d6), 9.32/10.27 (s, 1H); 8.82/8.88 (s, 1H); 7.74-7.82 (m, 1H); 7.30-7.38 (m, 1H); 7.02-7.19 (m, 1H); 6.61 (s, 2H); 5.40/5.62 (s, 2H). Anal. Calcd for $C_{11}H_9F_2N_7O_3$: C, 40.12; H, 3.07; N, 28.91. Found: C, 40.18; H, 3.00; N, 29.00.

2-(1-(2,4-difluorophenyl)-2-(3-nitro-1*H*-1,2,4-triazol-1-yl)ethylidene)hydrazine-1-carbothioamide (**4b**): (E:Z proportion = 79:31) Off-white powder, Yield: 60%, Temperature of decomposition: 211 ºC. IR (cm^{-1}): 1605 (C=N), 1508 (Ar-NO_2), 1365 (Ar-NO_2). ^{1}H NMR (DMSO-d_6): 10.31/11.17 (s, 1H); 8.85/8.91 (s, 1H); 8.43/8.56 (s, 1H); 7.83/8.06 (s, 1H); 7.06-7.45 (m, 3H); 5.47/5.75 (s, 2H). ^{13}C NMR (DMSO-d_6), 75 MHz: 179.48; 165.31; 162.00; 157.99; 147.63; 138.17; 131.32/132.44; 114.94/119.88; 112.60; 109.94; 55.47/48.08. Anal. Calcd for $C_{11}H_9F_2N_7O_2S$: C, 38.63; H, 2.64; N, 28.95. Found: C, 38.72; H, 2.56; N, 28.81.

2-(1-(2,4-difluorophenyl)-2-(1*H*-1,2,4-triazol-1-yl)ethylidene)hydrazine-1-carboxamide (**7a**): (*E:Z* proportion = 82:18) Off-white powder, Yield, 19%, Hygroscopic. ^{1}H NMR (DMSO-d$_6$): 10.20/9.21 (s, 1H); 8.55/8.44 (s, 1H); 7.91/7.94 (s, 1H); 7.65-7.73 (m, 1H); 7.08-7.34 (m, 2H); 6.57/6.41 (s, 2H); 5.51/5.28 (s, 2H). Anal. Calcd for $C_{11}H_{10}F_2N_6O$: C, 45.99; H, 3.88; N, 28.65. Found: C, 46.24; H, 3.81; N, 28.72.

2-(1-(2,4-difluorophenyl)-2-(1*H*-1,2,4-triazol-1-yl)ethylidene)hydrazine-1-carbothioamide (**7b**): (*E:Z* proportion = 58:42) Brown powder, Yield, 19%, Temperature of decomposition: 130 ºC. ^{1}H NMR (DMSO-d6): (E) 10,24/11,15 (s, 1H); 8,49/8,59 (s, 1H); 8,48/8,56 (s, 1H); 7,96/8,37 (s, 1H); 7,92/8,01 (s, 1H); 7,78-7,86 (m, 1H); 7,08-7,39 (m, 2H); 5,36/5,63 (s, 2H). .Anal. Calcd for $C_{11}H_{10}F_2N_6S$: C, 47.62; H, 4.45; N, 22.72. Found: C, 47.13; H, 4.33; N, 23.13.

Computational method

Geometry optimizations and energy calculations of compounds **4a**, **4b**, **7a** and **7b** were carried out at B3LYP and MP2 level applying cc-pVTZ[28] as basis set using the Gaussian09 suit of programs[29]. In order to study the solvent influence in the isomers energy, geometry optimizations were performed using SMD model[30] at MP2/cc-pVTZ and B3LYP/cc-pVTZ[28] level.

T. cruzi in vitro assay

The assay was performed as previously reported[7]. Briefly, on day 1 of the experiment, U2OS cells were seeded in black μClear 384-well tissue culture treated polystyrene plates

(Greiner Bio-One) at ratio of 700 cells in 40 µl of high glucose DMEM media (Hyclone) supplemented with 10% of heat inactivated fetal bovine serum, 100 µg/mL penicillin and 100 U/mL streptomycin (all reagents supplied by Gibco). Dispensing of cell suspension was performed with the aid of a Wellmate Liquid Handler (Thermo-Scientific). Plates were incubated for 24 h at 37 ºC/5% CO_2.

On day 2, trypomastigotes were harvested from the supernatant of LLC-MK_2 cell cultures infected with *T. cruzi* Y strain and added to the U2OS-containing 384 microplate at 2800 trypomastigotes in 10 µl of low glucose DMEM media (supplemented with 2% of heat inactivated fetal bovine serum – Gibco). On day 3, compounds were serially diluted by a factor of 2 (i.e. in 2-fold serial dilutions) in 100% DMSO in 15 dilution points in a polypropylene 384 well plate (Greiner BioOne) using a 16-channel manual pipette equipped with disposable tips (ThermoScientific), followed by transfer of 10 µL of compound solution onto assay plates, yielding a final concentration of 1% DMSO and a final volume of 60 µl/well. After 96 h, the plates were fixed for 15 min with 4% paraformaldehyde followed by 3 times washing with PBS and stained with 5 µM Draq5 (Biostatus) in DPBS. The highest compound concentration tested was 200 µM for test compounds, 400 µM for benznidazole and 100 µM for nifurtimox. The compounds were tested in two sets of experiments. In the first experiment, benznidazole was used as a control compound for evaluation of antiparasitic activity of compounds 3, 4a, 4b, and 7b, while nifurtimox was used as control for the test of compounds 6 and 7a in the second set of experiments. Each compound concentration was tested in doublets (i.e.. two wells per plate) and each experiment was performed in triplicate (i.e.. three independent experiments).

The plates were imaged in the High Content Analysis System Operetta (Perkin Elmer) with a 20x WD objective and images were analyzed with the High Content Analysis (HCA) software

Harmony (Perkin Elmer). This automated HCA protocol identifies, segment and quantitate for identification, segmentation and quantitation of host cell nuclei, cytoplasm and intracellular parasite based on the DNA staining. The HCA provides as output data for all images from one well: the total number of cells, total number of infected cells, total number of intracellular parasites and average number of parasite per infected cell.

Data analysis was performed as described elsewhere[7]. The infection ratio (IR) is the ratio of infected cells in a given population, and was determined as the ratio between the total number of infected cells and the total number of cells in in the test condition. The raw data for IR values was normalized to negative (infected cells, DMSO-treated) and positive (not infected cells, DMSO-treated) controls to determine the normalized antiparasitic activity.

Normalized activity values were processed with the Graphpad Prism software – version 6, for generation of sigmoidal dose-response (variable slope) nonlinear curve fitting and determination of EC_{50} and CC_{50} values by interpolation. The software also outputs maximum compound activity (Max. Actv.), calculated based on mean top normalized activity values provided by sigmoidal-curve fitting. For the purpose of this study, EC_{50} was defined as the compound concentration corresponding to 50% normalized activity after 96 h of compound incubation. Potency is used in reference to EC_{50} values (ie., the concentration of compound that reduces infection by 50% in comparison to controls), whereas efficacy relates to the maximum observed activity of a compound, regardless of the concentration. Cytotoxicity was measured by the CC_{50} value, defined as the compound concentration corresponding to reduction of 50% in the number of cells in comparison with negative controls (DMSO-treated, infected cells). A plate was assayed only with non-infected U2OS cells and compounds in order to compare CC_{50} values with those observed in infected cells. The selectivity index (S.I.) is a ratio between the value of

CC_{50} and EC_{50} and indicates the selectivity of biological activity towards the parasite; whenever CC_{50} cannot be calculated, the S.I. value was estimated as a ratio between the highest compound concentration tested and the EC_{50}.

AUTHOR CONTRIBUTIONS

Fredson T. Silva – Design, synthesis, chemical analysis of the compounds, molecular modeling calculations, text elaboration

Caio H. Franco – Anti-trypanosomal and cytotoxicity assays, text elaboration

Denize C. Favaro – Nuclear Magnetic Resonance and Molecular modeling calculations

Carolina B. Moraes - Anti-trypanosomal and cytotoxicity experiments supervisor, data analysis, text review

Lucio H. Freitas-Junior - Anti-trypanosomal and cytotoxicity experiments supervisor

Elizabeth I. Ferreira – General supervisor, MSc. student F. T. Silva supervisor, overall manuscript review, corresponding author

CONCFLICT OF INTEREST

All authors declare there is no conflict of interest at all.

ACKNOWLEDGEMENT

The authors thank FAPESP for F. T. Silva scholarship and funding of computational analysis facilities (2011/11499-0, 2011/17357-3, 2012/21865-7), and also to CNPq for E. I. Ferreira research fellowship.

REFERENCES

(1) Dias, J. C.P.; Silveira, A. C.; Schofield, C. J. The impact of Chagas disease controle in Latin America: a review. Mem. Inst. Oswaldo Cruz, **2002**, 97, 603-612.

(2) Chagas, C. Nova tripanozomiaze humana: estudos sobre a morfolojia e o ciclo evolutivo do Schizotrypanum cruzi n. gen., n. sp., ajente etiolojico de nova entidade morbida do homem. *Mem. Inst. Oswaldo Cruz.* **1909**, 2, 159-218.

(3) World Health Organization, WHO (2015). http://www.who.int/neglected_diseases/9789241564861/en/

(4) Cruz-Pacheco, G.; Esteva, L.; Vargas, C. Control measures for Chagas disease. *Math. Biosci.* **2012**, 237, 49-60.

(5) Dias, J. C. P. Cecilio Romaña, o sinal de Romaña e a Doença de Chagas. *Rev. Soc. Bras. Med. Trop.* **1997**, 30, 407-413.

(6) Urbina, J. A. Specific chemotherapy of Chagas disease: relevance, current limitations and new approaches. *Acta Trop.* **2010**, 115, 55-68.

(7) Moraes, C. B.; Giardini, M. A.; Kim, H.; Franco, C. H.; Araujo-Junior, A. M.; Schenkman, S.; Chatelain, E.; Freitas-Junior, L. H. Nitroheterocyclic compounds are more efficacious than

CYP51 inhibitors against *Trypanosoma cruzi*: implications for Chagas disease drug discovery and development. *Sci. Rep.* **2014**, 4 (4703), 1-11.

(8) Boveris, A.; Sies, H.; Martino, E. E.; Turrens, J. F.; Stoppani, A. O. Deficient metabolic utilization of hydrogen peroxide in *Trypanosoma cruzi. Biochem. J.* **1980**, 188, 643-648.

(9) Fairlamb, A. H.; Cerami, A. Metabolism and functions of trypanothione in the Kinetoplastida. *Annu. Rev. Microbio.* **1992**, 46, 695-729.

(10) Trossini, G. H. G.; Malvezzi, A.; T-do Amaral, A.; Rangel-Yagui, C. O.; Izidoro, M. A.; Cezari, M. H.; Juliano, L.; Chin, C. M.; Menezes, C. M.; Ferreira, E. I. Cruzain inhibition by hydroxymethylnitrofurazone: investigation of a new target in *Trypanosoma cruzi. J. Enzyme Inhib. Med. Chem.* **2010**, 25, 62-67.

(11) Xiao, L.; Madison, V.; Chau, A. S.; Loebenberg, D.; Palermo, R. E.; McNicholas, P. M. Three-dimensional models of wild-type and mutated forms of cytochrome P450 14alpha-sterol demethylases from *Aspergillus fumigatus* and *Candida albicans* provide insights into posaconazole binding. *Antimicrob. Agents Chemother.* **2004**, 48, 568-574.

(12) Sun, Q.; Xu, J.; Cao, Y.; Zhang, W.; Wu, Q.; Zhang, D.; Zhang, J.; Zhao, H.; Jiang, Y. Synthesis of novel triazole derivatives as inhibitors of P450 14 alpha-demethylase (CYP51). *Eur. J. Med. Chem.* **2007**, 42, 1226-1233.

(13) Lepesheva, G. I.; Zaitseva, N. G.; Nes, W. D.; Zhou, W.; Arase, M.; Liu, J.; Hill, G. C.; Waterman, M. R. CYP51 from *Trypanosoma cruzi*: a phyla-specific residue in the B' helix defines substrate preferences of sterol 14alpha-demethylase. *J. Biol. Chem.* **2006**, 281, 3577-3585.

(14) Barreiro, E. J.; Fraga, C. A. M. *Química Medicinal:* as bases moleculares da ação dos fármacos, 2 ed., Artmed: Porto Alegre, **2008**, pp. 271-277, 343-345.

(15) Lima, L. M.; Barreiro, E. J. Bioisosterism: a useful strategy for molecular modification and drug design. *Curr. Med. Chem.* **2005**, 12, 23-49.

(16) Viegas-Junior, C.; Danuello, A.; Bolzani, V. S.; Barreiro, E. J.; Fraga, C. A. M. Molecular hybridization: a useful tool in the design of new drug prototypes. *Curr. Med. Chem.* **2007**, 14, 1829-1852.

(17) Du, X.; Guo, C.; Hansell, E.; Doyle, P. S.; Caffrey, C. R.; Holler, T. P.; McKerrow, J. H.; Cohen, F. E. Synthesis and structure-activity relationship study of potent trypanocidal thio semicarbazone inhibitors of the trypanosomal cysteine protease cruzain. *J. Med. Chem.* **2002**, 45, 2695-2707.

(18) Portal, P.; Fernández, V. S.; Alonso, G. D.; De Vas, M. G.; Flawiá, M. M.; Torres, H. N.; Paveto, C. Multiple NADPH-cytochrome P450 reductases from *Trypanosoma cruzi* suggested role on drug resistance. *Mol. Biochem. Parasitol.* **2008**, 160, 42-51.

(19) Buckner, F. S.; Urbina, J. A. Recent developments in sterol 14alpha-demethylase inhibitors for Chagas disease. *Int. J. Parasitol. Drugs Dru. Resist.* **2012**, 2, 236-242.

(20) Rao, K. E.; Krowicki, K.; Burckhardt, G.; Zimmer, C.; Lown, J. W. Molecular recognition between oligopeptides and nucleic acids: DNA binding selectivity of a series of 1,2,4-triazole-containing lexitropsins. *Chem. Res. Toxicol.* **1991**, 4, 241-252.

(21) Landge, S. M.; Tkatchouk, E.; Benítez, D.; Lanfranchi, D. A.; Elhabiri, M.; Goddard, W. A.; Aprahamian, I. Isomerization mechanism in hydrazone-based rotary switches: lateral shift, rotation, or tautomerization? *J. Am. Chem. Soc.* **2011**, 133, 9812-9823.

(22) Jakusová, K.; Gáplovský, M.; Donovalová, J.; Cigán, M.; Stankovicová, H.; Sokolík, R.; Gaspar, J.; Gáplovský, A. Effect of reactants' concentration on the ratio and yield of *E,Z* isomers of isatin-3-(4-phenyl)semicarbazone and *N*-methylisatin-3-(4-phenyl)semicarbazone. *Chem. Pap.* **2013**, 67, 117-126.

(23) E. D. Glendening, J, K. Badenhoop, A. E. Reed, J. E. Carpenter, J. A. Bohmann, C. M. Morales, C. R. Landis, and F. Weinhold. *NBO 6.0.* Theoretical Chemistry Institute, University of Wisconsin, Madison, USA.

(24) Bosquesi, P. Planejamento, síntese e avaliação biológica de derivados furoxânicos e benzofuroxânicos potencialmente antichagásicos. Faculdade de Ciências Farmacêuticas. Programa de Pós Graduação em Ciências Farmacêuticas, **2013**.

(25) Moreno, M.; D'Avila, D. A.; Silva, M. N.; Galvão, L. M. C.; Macedo, A. M.; Chiari, E.; Gontijo, E. D.; Zingales, B. *Trypanosoma cruzi* benznidazole susceptibility in vitro does not predict the therapeutic outcome of human Chagas disease. *Mem. Inst. Oswaldo Cruz,* **2010**, 7, 918-924.

(26) Kazhemekaite, M.; Yuodvirshis, A.; Vektarene, A. Preparation of the pure sodium salt of 1H-1,2,4-triazole. *Chem. Heterocycl. Comp.* **1998**, 34, 277-278.

(27) Papadopoulou, M. V.; Bloomer, W. D.; Rosenzweig, H. S.; Chatelain, E.; Kaiser, M.; Wilkinson, S. R.; McKenzie, C.; Ioset, J. R. Novel 3-nitro-1H-1,2,4-triazole-based amides and sulfonamides as potential antitrypanosomal agents. *J. Med. Chem.* **2012**, 55, 5554-5565.

(28) Kendall, R. A.; Dunning Jr., T. H.; Harrison, R. J. Electron affinities of the first-row atoms revisited. Systematic basis set and wave functions. *J. Chem. Phys.* **1992**, 96, 6796-6806.

(29) Gaussian 03, Revision C.02, Frisch, M. J.; Trucks, G. W.; Schlegel, H. B.; Scuseria, G. E.; Robb, M. A.; Cheeseman, J. R.; Montgomery, Jr., J. A.; Vreven, T.; Kudin, K. N.; Burant, J. C.; Millam, J. M.; Iyengar, S. S.; Tomasi, J.; Barone, V.; Mennucci, B.; Cossi, M.; Scalmani, G.; Rega, N.; Petersson, G. A.; Nakatsuji, H.; Hada, M.; Ehara, M.; Toyota, K.; Fukuda, R.; Hasegawa, J.; Ishida, M.; Nakajima, T.; Honda, Y.; Kitao, O.; Nakai, H.; Klene, M.; Li, X.; Knox, J. E.; Hratchian, H. P.; Cross, J. B.; Bakken, V.; Adamo, C.; Jaramillo, J.; Gomperts, R.; Stratmann, R. E.; Yazyev, O.; Austin, A. J.; Cammi, R.; Pomelli, C.; Ochterski, J. W.; Ayala, P. Y.; Morokuma, K.; Voth, G. A.; Salvador, P.; Dannenberg, J. J.; Zakrzewski, V. G.; Dapprich, S.; Daniels, A. D.; Strain, M. C.; Farkas, O.; Malick, D. K.; Rabuck, A. D.; Raghavachari, K.; Foresman, J. B.; Ortiz, J. V.; Cui, Q.; Baboul, A. G.; Clifford, S.; Cioslowski, J.; Stefanov, B. B.; Liu, G.; Liashenko, A.; Piskorz, P.; Komaromi, I.; Martin, R. L.; Fox, D. J.; Keith, T.; Al-Laham, M. A.; Peng, C. Y.; Nanayakkara, A.; Challacombe, M.; Gill, P. M. W.; Johnson, B.; Chen, W.; Wong, M. W.; Gonzalez, C.; and Pople, J. A.; Gaussian, Inc., Wallingford CT, **2004**.

(30) Marenich, A. V.; Cramer, C. J.; Truhlar, D. G. Universal solvation model based on solute electron density and on a continuum model of the solvent defined by the bulk dieletric constant and atomic surface tensions. *J. Phys. Chem. B.* **2009**, 113, 6378-6396.

HIGHLIGHTS

- Four novel trypanomicidal non-toxic compounds are proposed.
- A novel compound showed promising EC_{50} value.
- The ratio of *Z* isomer of compounds increases with time due to mesomeric stabilization.